

# Direct Flux and Torque Control of Induction Motor Drive Changing the Hysteresis Band Amplitude

Lokanatha Dhall Samanta<sup>1</sup>, Bibhuti Bhusan Pati<sup>2</sup>, Bibhu Prasad Panigrahi<sup>3</sup>

Associate Professor, Dept. of Electrical Engg., SIET, Dhenkanal, Odisha, India<sup>1</sup>

Professor, Dept. of Electrical Engg., VSS University of Technology, Burla, Odisha, India<sup>2</sup>

Professor, Dept. of Electrical Engg., Indira Gandhi Institute of Technology, Sarang, Odisha, India<sup>3</sup>

**Abstract:** Direct Flux and torque control (DTC) based speed control strategy of induction motor (IM) drive and the effect of flux and torque hysteresis band amplitude on this strategy is presented. This scheme is simple and provides a good dynamic response. But the major problem associated with this DTC drive is high torque along with stator flux ripples. The direct torque control of induction machine is based on the use of two hysteresis controllers. The scheme for a 5 hp IM drive is simulated by changing the hysteresis band amplitude.

**Keywords:** DTC, hysteresis controller, induction motor drive, stator flux ripples, torque ripples, voltage source inverter (VSI).

## I. INTRODUCTION

Speed Control of IM by DTC, due to its simple structure and ability to achieve fast response of flux and torque has attracted growing interest in recent years. In direct torque controlled IM drives, it is possible to control directly the stator flux linkages and electromagnetic torque by selection of an optimum inverter switching table [1-2]. The switching table is selected to restrict the flux and torque errors within their respective hysteresis bands. Basically DTC utilizes two and three levels hysteresis band comparators for flux and torque control respectively. Unlike the field-oriented control (FOC) [3] this scheme does not need any coordinate transform and is less sensitive to motor parameter variation as only the stator resistance is required to estimate the flux and torque. The major drawback of DTC drive is the presence of steady state ripples in torque and flux. The pulsation in flux and torque affect the accuracy of speed estimation [4-5]. Here, a switching table based DTC scheme is presented. The flux and torque hysteresis band width is varied and it was observed that the width of the hysteresis band influence the drive performance in terms of current harmonics, torque ripple and switching frequency of the device [6-7]. For a fixed torque hysteresis band, as the flux band is increased the flux locus approaches a hexagonal shape due to harmonic distortion. On the other hand for a fixed flux hysteresis band if the torque hysteresis band amplitude is increased the torque ripple increases.

## II. DIRECT TORQUE CONTROL SCHEME

The switching table based DTC scheme uses stored switching information in a switching table, where the variables are flux and torque errors and the spatial position of flux vector linking the stator winding.

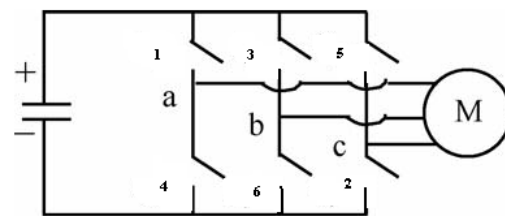


Fig. 1 Three phase inverter for DTC drive

### A. Flux and torque estimation

Stator flux based calculator method is used for calculating the electromagnetic torque, using only the stator flux linkages and stator currents. Only the stator resistance is employed in the computation of stator flux linkages, thereby removing the dependence of mutual and rotor inductances of the machine on its calculation.

As from Fig.1. the three phase inverter output voltages  $V_{as}$ ,  $V_{bs}$ ,  $V_{cs}$  and currents  $i_{as}$ ,  $i_{bs}$ ,  $i_{cs}$  are transformed into two phase stationary 'd' and 'q' axes voltages and currents as shown in Eqns. (1)-(4).

$$V_{qs} = V_{as} \quad (1)$$

$$V_{ds} = \frac{1}{\sqrt{3}}(V_{cs} - V_{bs}) \quad (2)$$

$$i_{qs} = i_{as} \quad (3)$$

$$i_{ds} = \frac{1}{\sqrt{3}}(i_{cs} - i_{bs}) \quad (4)$$

The stator d- and q-axis flux linkages [8] are given by Eqns. (5) and (6), where stator resistance drop has been compensated.

$$\lambda_{qs} = \int (V_{qs} - R_s i_{qs}) dt \quad (5)$$

$$\lambda_{ds} = \int (V_{ds} - R_s i_{ds}) dt \quad (6)$$

The resultant flux is given by Eqns. (7) and (8). The developed electromagnetic torque 'T<sub>e</sub>' is given by Eqn. (9).

$$\lambda_s = \sqrt{\lambda_{qs}^2 + \lambda_{ds}^2} < \theta_{fs} \quad (7)$$

$$\theta_{fs} = \tan^{-1}\left(\frac{\lambda_{qs}}{\lambda_{ds}}\right) \quad (8)$$

$$T_e = \frac{3}{2} * \frac{P}{2} (i_{qs} \lambda_{ds} - i_{ds} \lambda_{qs}) \quad (9)$$

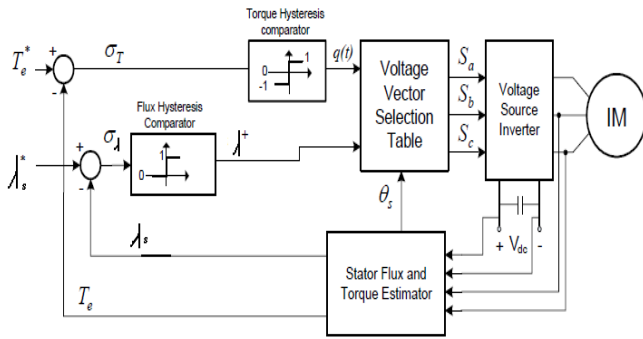


Fig. 2 Basic DTC structure

**B. Direct flux control**

As per Fig. 2 the resultant stator linked flux λ<sub>s</sub> is compared with the reference flux magnitude and the difference between the reference value and the estimated value gives the flux error which is given as input to the flux hysteresis comparator. In DTC the stator flux is forced to follow a circular locus by limiting its magnitude within the hysteresis band. When the stator flux touches its upper or lower hysteresis band, a suitable voltage vector is selected to reduce or increase it respectively. The output of the flux hysteresis comparator is the flux error status S<sub>λ</sub>. When S<sub>λ</sub> is '1' it calls for increase in flux and '0' for decrease in flux. In order to select the appropriate voltage vector the stator flux orientation or position must be known. The stator flux plane is divided into six sectors. Each sector will have a different set of voltage vectors to increase or decrease the flux.

**C. Direct torque control**

The estimated torque from the stator flux linkages and stator currents in Eqn. (9) is compared with the command torque. Depending on the torque error the torque can be increased or decreased by selecting suitable voltage vectors. The torque error has to be limited within its hysteresis band. The output of the torque hysteresis comparator is the torque error status S<sub>T</sub>. when it is '1' it calls for control action to increase torque, '-1' to decrease and '0' to maintain as it is.

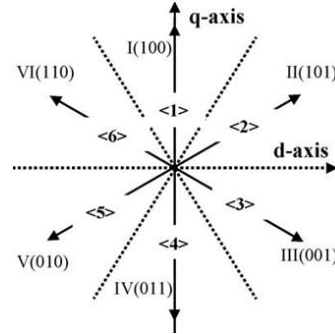


Fig. 3 Space voltage vectors and spatial sectors

**D. Formulation of the switching table**

Combining the flux error status output S<sub>λ</sub>, torque error status output S<sub>T</sub>, and the sextant of the flux phasor S<sub>θ</sub>, a switching table is realized to obtain the switching states of the inverter, given in Table I and the algorithm for S<sub>θ</sub> is shown in Table II.

TABLE I  
DTC SWITCHING TABLE

S <sub>λ</sub>	S <sub>T</sub>	S <sub>θ</sub>					
		<1>	<2>	<3>	<4>	<5>	<6>
1	1	110 (VI)	100 (I)	101 (II)	001 (III)	011 (IV)	010 (V)
1	0	111 (VIII)	000 (VII)	111 (VIII)	000 (VII)	111 (VIII)	000 (VII)
1	-1	101 (II)	001 (III)	011 (IV)	010 (V)	110 (VI)	100 (I)
0	1	010 (V)	110 (VI)	100 (I)	101 (II)	001 (III)	011 (IV)
0	0	000 (VII)	111 (VIII)	000 (VII)	111 (VIII)	000 (VII)	111 (VIII)
0	-1	001 (III)	011 (IV)	010 (V)	110 (VI)	100 (I)	101 (II)

TABLE II  
FLUX-PHASOR SEXTANT LOGIC (S<sub>θ</sub>)

θ <sub>fs</sub>	Sextant
0 ≤ θ <sub>fs</sub> ≤ π/3	<2>
-π/3 ≤ θ <sub>fs</sub> ≤ 0	<3>
-2π/3 ≤ θ <sub>fs</sub> ≤ -π/3	<4>
-π ≤ θ <sub>fs</sub> ≤ -2π/3	<5>
2π/3 ≤ θ <sub>fs</sub> ≤ π	<6>
π/3 ≤ θ <sub>fs</sub> ≤ 2π/3	<1>

Based on the three input variables ( $S_\lambda$ ,  $S_T$ ,  $S_0$ ), the required inverter output vector is specified in the above table using roman numerals. The six active voltage vectors (I–VI) and the two null vectors (VII and VIII) are denoted by the corresponding switching pattern shown along with the numeral denoting space voltage vector. For example, active voltage vector VI will require, as per Fig.1, turning on of upper switches in legs ‘a’ and ‘b’ and lower switch in leg ‘c’. Fig. 3 shows the six active space vectors and all the six spatial sectors described before. Each voltage vector is situated in the center of the corresponding sector. As we move in anticlockwise direction in the d-q plane, the sectors <6>, <5>, <4>, <3>, <2> and <1> come in sequence. Sector <1> extends from  $60^\circ$  to  $120^\circ$  (from d-axis, in the anticlockwise direction) of Fig. 2 and so on.

**E. Effects of hysteresis band amplitude on the DTC drive performance**

The amplitude of the hysteresis band influence the drive performance in terms of current harmonics, flux and torque ripples and switching frequency of the device [6-7].

(a) Effects of flux hysteresis band amplitude  $\Delta\lambda$ : for a prefixed torque band amplitude, inverter switching frequency is related to the amplitude of flux hysteresis band. It is observed from the simulation result that a small flux band amplitude determines higher switching frequency. The stator flux vector locus approaches a circle and the phase current waveform is nearly sinusoidal. As the amplitude of the flux hysteresis band increases the switching frequency decreases and the stator flux vector locus degenerates to a hexagon and the phase current wave form is similar to six-step inverter-fed induction machine.

(b) Effects of torque hysteresis band amplitude  $\Delta T$ : the torque hysteresis band is varied from 5% to 25% of the torque limit allowed. From the simulation results it is observed that as the torque hysteresis band increases the torque ripple increases. On the other hand if the band amplitude is too small, a torque overshoot which may cause the torque error to exceed the hysteresis band will occur. This will result in a reverse voltage vector to be selected (instead of a zero vector) to reduce the torque [9]. A reverse voltage vector will reduce the torque rapidly and hence may in turn cause a torque overshoot and consequently torque ripple is reduced.

**III. SIMULATION RESULTS**

The complete simulation model of the DTC based induction motor drive is developed using Matlab/Simulink. The nominal motor parameters are mentioned in Appendix. Sample simulation results are presented below. Figs. 4(a) and 4(b) show the stator flux vector locus and stator current waveform respectively for a flux hysteresis band of amplitude 0.01 Wb. Fig. 5(a) and 5(b) show the stator flux vector locus and stator current waveform for a flux hysteresis band of amplitude 0.1 Wb. For both the cases the torque hysteresis band is kept constant at 0.05 N-m. Figs.

6(a) and 6(b) show the developed electromagnetic torque waveform and the stator current waveform for a torque hysteresis band of amplitude 1 N-m. Similarly Figs. 7(a) and 7(b) demonstrate the torque and current waveform for a torque hysteresis band of amplitude 2 N-m. and the flux hysteresis band amplitude is kept constant at 0.02 Wb in both the cases.

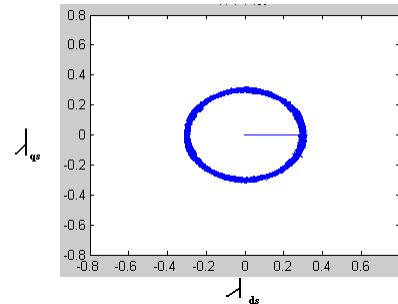


Fig. 4(a) Stator flux vector locus for  $\Delta\lambda=0.01$  Wb

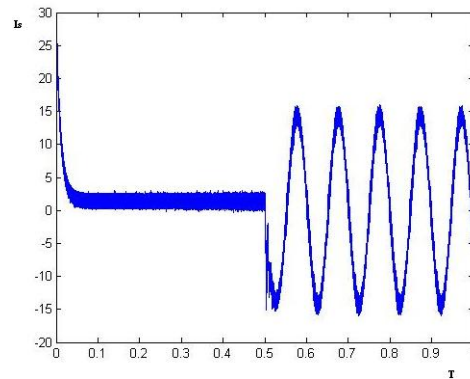


Fig. 4(b) Stator current Vs Time plot

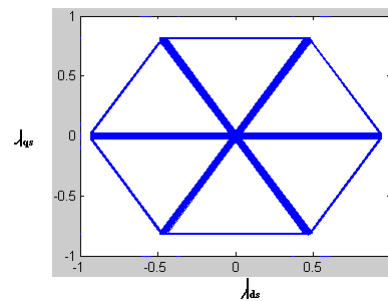


Fig. 5(a) Stator flux vector locus for  $\Delta\lambda=0.1$  Wb

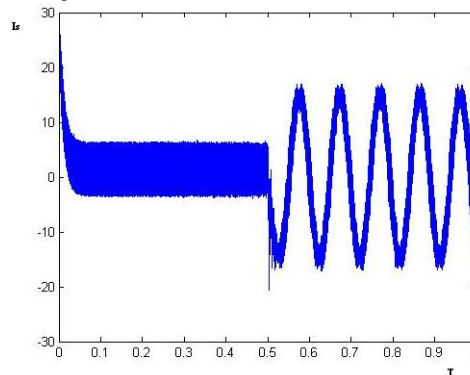


Fig. 5(b) Stator current Vs Time plot

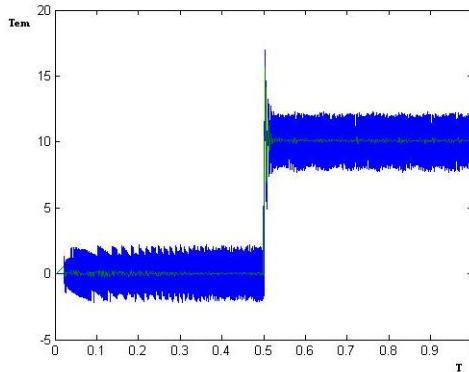


Fig. 6(a) Electromagnetic torque Vs Time plot for  $\Delta T=1N\text{-m}$

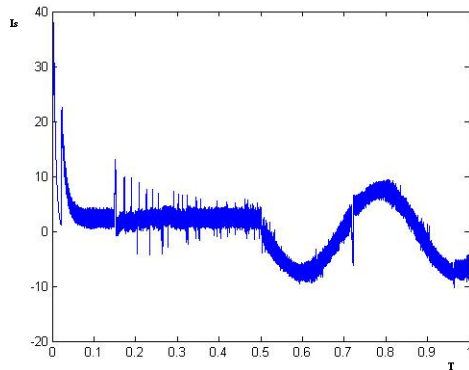


Fig. 6(b) Stator current Vs Time plot

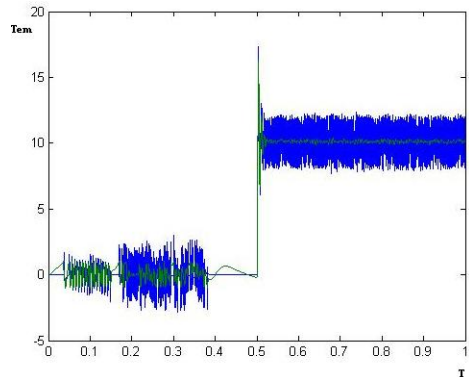


Fig. 7(a) Electromagnetic torque Vs Time plot for  $\Delta T=2N\text{-m}$

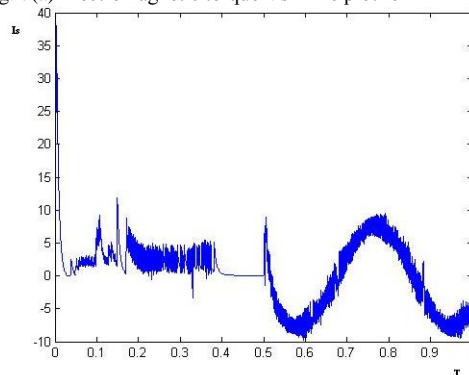


Fig. 7(b). Stator current Vs Time plot

#### IV. CONCLUSION

In this paper a switching table based direct torque control scheme for speed control of induction motor drive has been presented. The effect of amplitude of flux and torque hysteresis band on the flux vector locus and torque ripple of an IM is discussed. This scheme of speed control of IM using the hysteresis comparators has some drawbacks like the presence of flux and torque ripples. So selection of optimum amplitude of flux and torque hysteresis band is important for the drive.

#### Acknowledgment

The authors gratefully acknowledge the contributions of Department of Electrical Engg., VSSUT, Burla for extending their AICTE RPS Project facilities in carrying out the simulation work.

#### APPENDIX

The parameters of the induction motor used in simulation study are  $P=2$ ,  $R_s=1.115\Omega$ ,  $R_r=1.083\Omega$ ,  $V_{L-L}=460V$ ,  $L_s=5.974mH$ ,  $L_r=5.974mH$ ,  $L_m=0.2037H$ , rated frequency=60 Hz, rated speed=183rad/sec,  $T=20N\text{-m}$ ,  $P_{rated}=5hp$ ,  $J=0.02Kg\cdot m^2$ ,  $B_m=0.005752N\cdot m/rad/sec$ .

#### REFERENCES

- [1]Takahashi I., Nouguchi T., "A new quick response and high efficiency control strategy for an induction motor," IEEE Trans. Ind. Application. , 1986, Vol. 22, No. 5, pp.820-827.
- [2]M. Depenbrock., "Direct self-control (DSC) of inverter-fed induction machine," IEEE Trans. Power Electronics., Vol.3, No.4, October 1988, pp. 420-429.
- [3] D. Casadei, F. Profumo, G.Serra and A.Tani, " FOC and DTC: Two Viable Schemes for Induction Motors Torque Control", IEEE Trans.on Power Electronics., Vol.17, No.5, Sept 2002.pp.779-787
- [4] Isao Takahashi and Youichi Ohmori, "High Performance Direct Torque Control of an Induction Motor", IEEE Transactions on Industry Applications, Vol. IA-25, No.2, 1989, pp. 257-264.
- [5] D. Casadei and G.Serra and A.Tani "Implementation of Direct Torque Control Algorithm for Induction Motors Based On Discrete Space Vector Modulation", IEEE Trans. Power Electronics. Vol.15, No.4, JULY 2000, pp.769-777.
- [6] Jun-Koo Kang; Dae-Woong Chung; Seung-Ki Sul (1999). "Direct control of induction machine with variable amplitude control of flux and torque hysteresis bands", International Conference IEMD'99, pp. 640-642.
- [7] Casadei, D, Grandi, G., Serra, G. and Tani, A. (1994). "Effect of flux an torque hysteresis band amplitude in direct torque control of induction motor", in Conf. Rec. IEEE-IECON '94, pp. 299-304.
- [8] J. Luukko, M. Niemela, J. Pyrhonen, "Estimation of the flux linkage in a direct-torque-controlled drive", IEEE Trans. Ind. Electron, Vol. 50 No.2, 2003, pp.283-287.
- [9] Casadei, D., Grandi, G., Serra, G. and Tani, A.(1994). "Switching Strategies in direct torque control of induction machine", In Con. Rec. International Conf on Electrical Machines, Paris, France, 1994, pp. 204-209.